



Spatio-temporal analysis of rainfall extremes in the flood-prone Nagavali and Vamsadhara Basins in eastern India

G. Venkata Rao^a, K. Venkata Reddy^a, Raghavan Srinivasan^b, Venkataramana Sridhar^{c,*}, N. V. Umamahesh^a, Deva Pratap, Ph.D^a

^a Department of Civil Engineering, National Institute of Technology Warangal, Telangana, 506004, India

^b Director of Spatial Sciences Laboratory, Agrilife Research, Texas A&M University, College Station, TX, 77843, United States

^c Department of Biological Systems Engineering, Virginia Polytechnic Institute and State University, Blacksburg, VA, 24061, USA

ARTICLE INFO

Keywords:

Rainfall
Extremes
Mann-kendall test
Sen's slope
Kriging interpolation

ABSTRACT

Understanding the spatio-temporal distribution of rainfall characteristics has a major role in assessing the availability of water resources over a catchment. Therefore, it is necessary to understand the changes in rainfall characteristics using gridded precipitation data and robust statistical analysis for making decisions. In this study, the trends in rainfall and rainfall extremes over the Nagavali and Vamsadhara river basins are studied at three time steps (long-term-1901-2018, pre-1950, and post-1950) with four different Mann-Kendall (MK) tests using daily gridded rainfall data of 118 years (1901–2018). The spatial patterns of the trends are evaluated with the kriging interpolation method. Magnitude in rainfall and rainfall extremes (CDD, CWD, PRCPTOT, R10MM, R20MM, R40MM, R95PTOT, RX1DAY, and RX5DAY) are analyzed using the Sen's slope method. Except in the monsoon season, a decreasing trend is observed in all the rainfall extremes in post-1950 compared to pre-1950 period. Whereas, in the monsoon an increasing trend is observed for the extremes in post-1950 period. Overall period (i.e., 1901–2018) an increasing trend is observed for rainfall and rainfall extremes in the pre-monsoon (March–May), monsoon (June–Sep) seasons and a decreasing trend in the winter season (Dec–Feb) for both the basins. No obvious trends are evident in the post-monsoon season (Oct–Nov). At the annual scale, rainfall and rainfall extremes exhibited an increasing trend. Overall, the Nagavali basin experienced more extreme rainfall events indicating the higher vulnerability of floods while the middle and lower portions of the Vamsadhara basin shown increase in extremes. When linked with hydrological analysis, insights gained from this study are useful for flood vulnerability mapping and risk assessment for both the basins.

1. Introduction

The spatio-temporal variability of climate and climate drivers have caused changes in frequency and intensity of climate extremes such as floods, droughts and tropical cyclones which have significant impact on human life and socio-economic aspects of India (Jayadas and Ambujam, 2019). Rainfall is one of the most important climate variables that varies both in space and time, and its response in modifying the basin scale hydrological processes are critical for water resources management in a river basin (Seong and Sridhar, 2017; Sridhar et al., 2013; Weldegerima et al., 2018). The spatio-temporal distribution of rainfall would have a direct impact on the availability of water resources in a river or a catchment (Adarsh and Janga Reddy, 2015). The uneven distribution of

rainfall intensities leads to increased incidences of extreme events and their intensities which often lead to floods or droughts (Dhar and Nandargi, 2003; Guhathakurta et al., 2011). The changes in extremes can also be directly related to changes in mean climate, because mean future conditions in some variables are projected to lie within the tails of present day situation (Seneviratne and Nicholls, 2012). Therefore, there is a need to understand the characteristics of rainfall and rainfall extremes in a river basin to enhance the water resources management strategies.

Rainfall and extreme rainfall events were extensively studied in India at national and regional scales and have drawn different conclusions (Bisht et al., 2018a, 2018b; Dash et al., 2009; Deshpande et al., 2016; Dubey and Sharma, 2018; Ghosh et al., 2012; Goswami et al., 2006;

* Corresponding author.

E-mail addresses: gvenkat@student.nitw.ac.in (G. Venkata Rao), kvreddy@nitw.ac.in (K. Venkata Reddy), r-srinivasan@tamu.edu (R. Srinivasan), vsri@vt.edu (V. Sridhar), mahesh@nitw.ac.in (N.V. Umamahesh), prataprec@yahoo.com (D. Pratap).

<https://doi.org/10.1016/j.wace.2020.100265>

Received 5 January 2020; Received in revised form 5 May 2020; Accepted 25 May 2020

Available online 29 May 2020

2212-0947/© 2020 The Authors. Published by Elsevier B.V. This is an open access article under the CC BY license (<http://creativecommons.org/licenses/by/4.0/>).

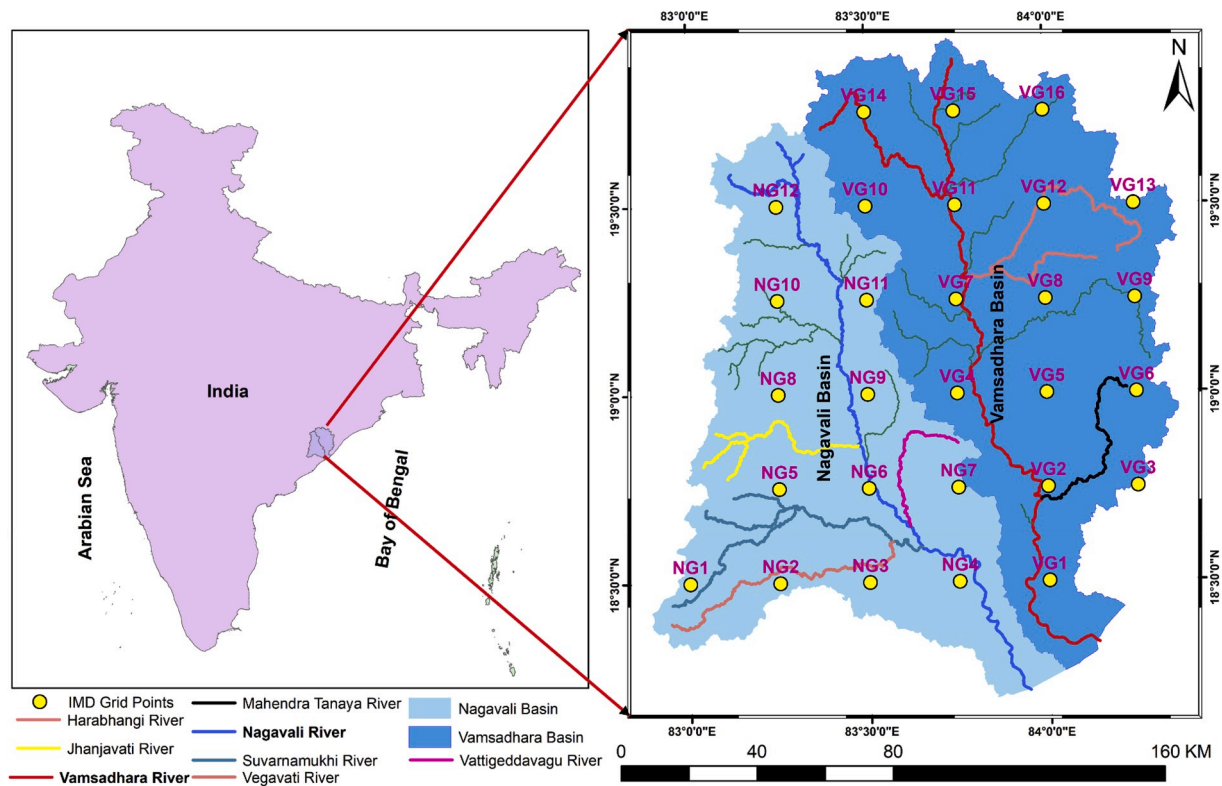


Fig. 1. Geographical Location of the Study Area (NG represents grid point over Nagavali basin and VG represents grid point over Vamsadhara Basin).

Guhathakurta et al., 2011, 2017; 2015; Guhathakurta and Rajeevan, 2008; Jain et al., 2017; Kumar et al., 2010; Rajeevan et al., 2008; Roy and Balling, 2004; Sharma et al., 2018). Some studies reported no clear long-term changes in rainfall over a period longer than a century at annual, seasonal and monthly time scale over India (Ghosh et al., 2012; Kumar et al., 2010; Rajeevan et al., 2008). However, Kumar et al. (2010) reported an increase in magnitudes of winter, pre and post monsoon rainfall and decrease in annual and monsoon rainfall at the national scale. At the same time, extreme rainfall events in India exhibited significant trends in their occurrence at various scales. Roy and Balling (2004) reported an increasing trend in rainfall extremes during the period 1910–2000 over the whole of India. Goswami et al. (2006) showed increasing trends for heavy rainfall events and decreasing trends in moderate events over central India during monsoon in the last half century (1951–2000). Rajeevan et al. (2008) reported a 6% increase per decade in rainfall extremes over the central parts of India during 1901–2004. Whereas, Guhathakurta et al. (2011) found that frequencies of extreme rainfall are decreasing in central and northern India and increasing in other parts of the country. Also, increasing heavy rainy days and decreases in moderate rainy days in the last half century was reported (Dash et al., 2009). Guhathakurta et al. (2015) reported that moderate events exhibited decreasing or no trends in frequencies of heavy or very heavy precipitation days during the monsoon over India from 1901 to 2011. In the monsoon season, the number of zero rainfall days were found to be increasing in major river basins of India (Deshpande et al., 2016; Dubey and Sharma, 2018; Sharma et al., 2018). However, the number of rainy days were increasing as reported by Jain et al. (2017) for the rivers flowing towards the east direction, suggesting that distinction should be drawn between the east and west flowing rivers when quantifying the trends in rainfall characteristics.

Majority of the previous studies to detect the trends in rainfall and rainfall extremes used the original Mann-Kendall (MK) test. The MK test has proven to be useful in determining the significant trends in hydrologic data at different probability levels (Bisht et al., 2018a; Yadav et al., 2014) which assumes spatial and temporal independence in

hydrological time series data (Adarsh and Janga Reddy, 2015; Deshpande et al., 2016; Dubey and Sharma, 2018; Guhathakurta et al., 2015). It is well documented that the presence of either positive or negative autocorrelation influences the significance of trend (Kumar et al., 2009). The original MK test assumes no serial correlation in the hydrological time series data. However, most often, hydrological time series data are autocorrelated and leads to a disproportionate false rejection of the null hypothesis (Hamed, 2008; Hamed and Rao, 1998; Yue et al., 2003). Similarly, the presence of long-term persistence can lead to underestimation of serial correlation and overestimation of the significance of trends (Su et al., 2018). To overcome these effects, trend analysis is performed in this study using four kinds of MK tests i.e., the original Mann-Kendall test (MK1), Mann-Kendall test with trend-free pre-whitening (MK2), modified Mann-Kendall test (MK3), and Mann-Kendall test with long-term persistence (MK4).

From the previous studies, it is clear that patterns and variability of rainfall characteristics at various temporal scales (i.e., annual, seasonal, and monthly) were widely investigated, while studies on rainfall extremes were limited to annual scales and for the monsoon period. Furthermore, only limited studies on monthly trends in rainfall extremes were available and no studies were performed for the winter, pre- and post-monsoon seasons. Bisht et al. (2018a) suggested that it is important to carry out trend analysis for rainfall characteristics for a basin at regional level rather than at national level for making better decisions. Along with the trend analysis, it is also very important to study the change point of the trend. The studies by Vittal et al. (2013) and Bisht et al. (2018a) reported that, urbanization in India has altered the significant trends in rainfall and rainfall extremes. Urbanization is the change point of climate change adaptation due to increase global warming (Sridhar et al., 2019). Vittal et al. (2013) has found significant changes in the patterns of rainfall extremes in post-1950 compared to pre-1950 period. Whereas, Bisht et al. (2018a) has reported significant changes in post-1975 compared to pre-1975. From these studies, it is difficult to know the exact time of change in trends. To overcome the difficulty, Pettit's test (Jaiswal et al., 2015) was performed over the

Table 1
Details of the gauge data in Nagavali and Vamsadhara basins.

Name of the Station	Latitude	Longitude	River Name	Data Availability	Data Type
Gunupur	19° 05' 00" N	83° 48' 20"E	Vamsadhara	01.05.1978–31.05.2019	Daily
Kasinagar	18° 50' 54" N	83° 52' 23"E	Vamsadhara	01.07.1980–31.05.2019	Daily
Gudari	19° 23' 00" N	83° 47' 32"E	Vamsadhara	01.05.1978–31.05.2019	Daily
Kutragada	19° 36' 40" N	83° 33' 52"E	Vamsadhara	01.07.1987–31.05.2019	Daily
Mahendragarh	19° 13' 24" N	84° 15' 45"E	Vamsadhara	01.07.1987–31.05.2019	Daily
Mohana	19° 26' 41"N	84° 15' 41"E	Vamsadhara	01.07.1987–31.05.2019	Daily
Gottabarrage	18° 42' 00"N	83° 58' 00"E	Vamsadhara	01.07.1987–31.05.2019	Daily
Srikakulam	18° 18' 48"N	85° 53' 03"E	Nagavali	01.03.1988–31.05.2019	Daily

Nagavali and Vamsadhara basins. The results are in good agreement with [Vittal et al. \(2013\)](#). Therefore, the hypothesis for this study is that the trends in rainfall and rainfall extremes for small river basins will be the same or differ, while generalizing from large river basin studies. No in-depth study on rainfall characteristics using long-term time series data is presently available for the two small river basins, Nagavali and Vamsadhara located between Godavari and Mahanadi basins in eastern India. Therefore, the present study aims to provide the comprehensive assessment of the trends in rainfall and rainfall extremes in three time periods i.e., long-term (1901–2018), pre-1950 (1901–1950), and post-1950 (1951–2018) for their better understanding in the Nagavali and Vamsadhara basins. In the following sections, study area, data, methodology and results are presented.

2. Study area

The Nagavali and Vamsadhara are two independent, adjacent and interstate eastern flowing rivers between Rushikulya and Godavari rivers in Odisha and Andhra Pradesh states in India ([Fig. 1](#)). The Nagavali and Vamsadhara rivers originate at Thuamul Rampur block of Kalahandi district of Odisha, flow through nine districts and drain into the Bay of Bengal at Bontala Koduru and Kalingapatnam in Andhra Pradesh, respectively. The total length of the Nagavali river is about 256 km long with a catchment area of 9510 km² and the Vamsadhara river is about 254 km long with a catchment area of 10830 km².

The Nagavali and Vamsadhara basins are divided into three parts such as lower, middle, and upper basins, respectively based on the spatial distribution of rainfall. The lower portion of the basin extends from the base of the Eastern Ghats to the coast. A total of 28 grids of rainfall data is falling over both the basins out of which 12 grids are over the Nagavali basin and the remaining over the Vamsadhara basin. The average annual rainfall over the Nagavali and Vamsadhara basins are 1230 mm and 1260 mm, respectively for 118 years (1901–2018). During every monsoon season, more than 150 villages and 1000 acres of crop fields in both the basins are facing a flood threat apart from the cyclones and thunderstorms in other seasons. Therefore, there is a need to understand the trends in rainfall and rainfall extremes over the Nagavali and Vamsadhara basins to enhance the water resources management strategies. This investigation is carried out as part of development of a framework for real-time forecasting of floods using the Soil and Water Assessment Tool (SWAT) over the Nagavali and Vamsadhara basins.

3. Data and methods

3.1. Data

Daily rainfall records for a period of 118 years (i.e., 1901–2018) from India Meteorological Department (IMD) are available in the gridded format at 0.25° spatial resolution. Monthly, seasonal and annual rainfall are derived from the daily rainfall records. More details about the data are reported in [Pai et al. \(2014\)](#). No missing data is observed in the daily time series. The rain gauge data for a period of more than 30 years for both the Nagavali and Vamsadhara basins was obtained from Mahanadi & Eastern Rivers Organization (M&ERO), Central Water Commission

Table 2
List of Rainfall extremes in the present study and their definitions (Source: http://etccdi.pacificclimate.org/list_27_indices.shtml).

Extremes	Units	Definitions
CDD	Day	Maximum length of dry spell, Maximum number of consecutive days with RR < 1 mm. Count the largest number of consecutive days where RR _{ij} < 1 mm
CWD	Day	Maximum length of wet spell, Maximum number of consecutive days with rainfall ≥ 1 mm. Count the largest number of consecutive days where RR _{ij} ≥ 1 mm
PRCPTOT	mm	Total amount of rainfall in wet days. If I represents the number of days in j, then PRCPTOT = ∑ _{j=1} ^I RR _{ij}
R10MM	Day	Number of days when RR ≥ 10 mm. Count the number of days where RR _{ij} ≥ 10 mm.
R20MM	Day	Number of days when RR ≥ 20 mm. Count the number of days where RR _{ij} ≥ 20 mm.
R40MM	Day	Number of days when RR ≥ nmm. Count the number of days where RR _{ij} ≥ nmm. (Where nn = User defined threshold)
R95PTOT	mm	Total rainfall when RR > 95p. Let RR _{wj} be the daily precipitation amount on a wet day w (RR ≥ 1 mm) in period I and let RR _{wn} be the 95th percentile of RR on wet days. If W represents the number of wet days in the period, then R95p _j = ∑ _{w=1} ^W RR _{wj} where RR _{wj} > RR _{wn} 95
RX1DAY	Day	Maximum 1-day rainfall. The maximum 1-day values for period j are RX1DAY _j = max (RR _{ij})
RX5DAY	Day	Maximum 5-day rainfall. Let RR _{kj} be the rainfall amount for the 5-day interval ending k period j. The maximum 5-day values for period j are RX5DAY _j = max (RR _{kj})

*RR_{ij} be the daily rainfall amount on the day i in period j.

(CWC) Bhubaneswar. The details of the gauge data are shown in [Table 1](#). As a quality control measure, the daily gridded rainfall data is compared with the gauge data and found a good correlation of 0.79 between them.

The rainfall extremes plays an important role in understanding their hydrological impacts in a river basin ([Yang et al., 2016](#)). Based on the daily values of temperature and precipitation, the joint CCI/WCRP/JCOMM Expert Team on Climate Change Detection and Indices (ETCCDI) defined a total of 27 indices out of which 11 for precipitation extremes and 16 for temperature extremes to gain insight to the changes in extremes ([Yang et al., 2016](#)). Among the 11 precipitation indices, 9 were selected to investigate the characteristics of rainfall extremes over the Nagavali and Vamsadhara basin. The details description of rainfall extremes are presented in [Table 2](#). The rainfall extremes were calculated at

Table 3
Data format for computing rainfall extremes.

Year	Jday	IMD Gridded Data
1901	1	0
1901	2	0
1901	3	0.7
1901	4	0
1901	5	3
1901	6	1.5
1901	7	2
1901	8	0

various temporal scales (i.e., monthly, seasonal, and annual) by using RClimDex package in R (Version 3.5.3) (Bronaugh, 2019) developed and maintained by Xuebin Zhang and Yang Fang at Climate Research Division (CRD) or ETCCDI. It is the most commonly used package for calculating the rainfall extremes. The package will also conducts the simple quality control on the input data before calculating the rainfall extremes. The data format for calculating the rainfall extremes is presented in Table 3. For calculating consecutive dry days (CDD), the software will count the number of consecutive days with rainfall less than 1 mm. From the data provided in Table 3, the CDD is 4 days.

3.2. Methodology

3.2.1. Mann-Kendall test (MK1)

The original Mann-Kendall (MK) (Kumar et al., 2009) test is widely used for detecting the trends in a hydrological time series dataset. If $x_1, x_2, x_3, \dots, x_n$ is the time series of length n , then the MK1 test statistics S is given as

$$S = \sum_{i=1}^n \sum_{j=i+1}^n \text{sign}(x_j - x_i) \quad (1)$$

where,

$$\text{sign}(x_j - x_i) = \begin{cases} 1 & \text{if } (x_j - x_i) > 0 \\ 0 & \text{if } (x_j - x_i) = 0 \\ -1 & \text{if } (x_j - x_i) < 0 \end{cases} \quad (2)$$

Null hypothesis (H_0): there is no trend in a hydrological time series dataset. Alternate hypothesis (H_1): there exists an increasing or decreasing trend in a hydrological time series dataset. As S is normally distributed the mean $E(S)$ and variance of $V(S)$ of statistic S in eq. (1) is given as

$$E(S) = 0 \quad (3)$$

$$V(S) = \frac{n(n-1)(2n+S)}{18} \quad (4)$$

The MK standardized test statistics Z is given by

$$Z = \begin{cases} \frac{S-1}{(V(S))^{1/2}} & S > 0 \\ 0 & S = 0 \\ \frac{S+1}{(V(S))^{1/2}} & S < 0 \end{cases} \quad (5)$$

The negative values of S indicates decreasing trend and vice versa. The test statistic Z gives significance levels (SL) of rejecting null hypothesis. Confidence level (CL) of rejecting the null hypothesis is given by

$$CL = 1 - SL \quad (6)$$

The magnitude of trends determined by the Theil-Sen approach (TSA) (Kumar et al., 2009). The TSA slope

$$\beta = \text{median} \left[\frac{x_j - x_i}{j - i} \right] \text{ for all } i < j \quad (7)$$

If the condition $-Z_{\frac{\alpha}{k}} \left(1 - \frac{\alpha}{k}\right) \leq Z_k \leq Z_{\frac{\alpha}{k}} \left(1 + \frac{\alpha}{k}\right)$ is satisfied then H_0 will be accepted with a significance level of α , otherwise, H_1 will be accepted.

3.2.2. Mann-Kendall test with trend-free pre-whitening (MK2)

Yue et al. (2003) recommended that there will be an increase (decrease) in S value when autocorrelation is positive (negative) which is underestimated (overestimated) by the original variance $V(S)$. Thus, when trend analysis is conducted for this data using MK-1, it will show positive or negative trends when actually there is no trend. So, trend free

pre-whitening treatment is adopted where lag-1 serial correlation components are removed from the series prior to applying of MK test for trend detection. Following steps are used to determine trend analysis using MK-2 test.

Calculate the lag-one ($k = 1$) autocorrelation coefficient (r_1) using

$$r_k = \frac{\frac{1}{n-k} \sum_{i=1}^{n-k} (x_i - \bar{x})(x_{i+k} - \bar{x})}{\frac{1}{n} \sum_{i=1}^n (x_i - \bar{x})^2} \quad (8)$$

If the condition $\frac{-1-1.645\sqrt{n-2}}{n-2} \leq r_1 \leq \frac{-1+1.645\sqrt{n-2}}{n-2}$ is satisfied, then the series is assumed to be independent at 10% significance level and there is no need of pre-whitening. Otherwise, pre-whitening is required for the series before applying MK-1 test.

Using eq. (9) remove the trend in time series data to get detrended time series. The value of β is obtained from eq. (7)

$$x_i' = x_i - (\beta \times i) \quad (9)$$

Using eq. (8) to calculate lag-1 autocorrelations for detrended time series given by x_i' . Using eq. (10) remove the lag-one autoregressive component (AR (1)) from the detrended series to get a residual series.

$$y_i' = x_i' - r_1 \times x_{i-1}' \quad (10)$$

Yet again, $(\beta \times i)$ value is added to the residual series as follows

$$y_i = y_i' + (\beta \times i) \quad (11)$$

The MK test is applied to the blended series Y_i to determine the significance of the trend.

3.2.3. Modified Mann-Kendall test 3 (MK3)

Sometimes removing lag-one autocorrelation is not enough for many hydrological time series datasets. Hamed and Rao (1998) proposed a modified Mann Kendall test where the effect of all significant autocorrelation coefficients are removed from a data set. The modified variance of S was used i.e., $V(S)^*$ instead of $V(S)$ which is given as follows:

$$V(S)^* = V(S) \frac{n}{n^*} \quad (13)$$

where n^* = effective sample size. Hamed and Rao (1998) proposed an equation for the calculation of $\frac{n}{n^*}$ given as

$$\frac{n}{n^*} = 1 + \frac{2}{n(n-1)(n-2)} \sum_{i=1}^n (n-1)(n-i-1)(n-i-2)r_i \quad (14)$$

where n = actual number of observations, r_i = lag- i significant autocorrelation coefficient of rank i of time series. After calculating $V(S)^*$ substitute it in place of $V(S)$ in eq. (4) when calculating the Z from eq. (5).

3.2.4. Mann-Kendall test with long-term persistence (MK4)

In addition to the lag-one autocorrelation i.e. short-term persistence, the presence of Long-Term Persistence (LTP) or the Hurst Phenomenon (H) (Hurst, 1951) can considerably influences the significance of trends in hydrological time series dataset. To overcome the LTP, considered the Mann Kendall test with LTP (Hamed, 2008). Following steps are used to determine trend analysis using MK-4 test.

3.2.5. Procedure for calculating Hurst Phenomenon (H)

A new time series x_i' is calculated from eq. (9). Using the ranks (R_i) of the detrended time series x_i' , Z variate is calculated as follows:

$$Z_i = \varnothing^{-1} \left(\frac{R_i}{n+1} \right) \quad (14a)$$

where n = observation size, \varnothing^{-1} = inverse of standard normal distribution function with zero mean and standard deviation = 1.

For a given H , calculate the elements of the Hurst matrix as follows

$$C_n(H) = [\rho_{|j-i|}] \text{ for } i = 1:n, j = 1:n \tag{15}$$

where ρ_l represents lag-1 autocorrelation coefficient given as

$$\rho_l = \frac{1}{2} [|l+1|^{2H} - 2|l|^{2H} + |l-1|^{2H}] \text{ for } l > 1 \tag{16}$$

To calculate the exact value of H, the maximizing likelihood function is used

$$\log L(H) = -\frac{1}{2} \log |C_n(H)| - \frac{Z^T [C_n(H)]^{-1} Z}{2\gamma_0} \tag{17}$$

where transpose of $Z (Z^T)$ is obtained from MK-1 test, $C_n(H)$ is the Hurst matrix, γ_0 represents the variance. The eq (17) is solved for different values of H ranging from 0.5 to 0.98 with 0.01 step interval and the H value which produces maximum $L(H)$ detected as answer.

The mean and Standard Deviation of H in terms of n (Hamed, 2008) are as follows:

$$\mu_H = 0.5 - 2.87n^{-0.9067} \tag{18}$$

$$\sigma_H = 0.77654n^{-0.5} - 0.0062 \tag{19}$$

Then calculate $Z_c = \frac{H-\mu_H}{\sigma_H}$ for the significance of trend at 10% significance level.

For significant H, calculate the modified variance for S, recommended by Kumar et al. (2009).

$$V(S)^H = \sum_{i<j} \sum_{k<l} \frac{2}{\pi} \sin^{-1} \left(\frac{\rho|j-l| - \rho|i-l| - \rho|j-k| + \rho|i-k|}{\sqrt{(2-2\rho|i-j|)(2-2\rho|k-l|)}} \right) \tag{20}$$

where ρ_l is calculated from eq. (16).

As the modified variance ($V(S)^H$) is a biased estimator, correction is needed for bias as follows

$$V(S) = V(S)^H \times b \tag{21}$$

where

$$b = a_0 + a_1H + a_2H^2 + a_3H^3 + a_4H^4 \tag{22}$$

$a_0, a_1, a_2, a_3,$ and a_4 are coefficients which depends on the number of observations as given by Kumar et al. (2009). The modified variance $V(S)^H$ obtained from eq. (20) was substituted in place of V(S) (eq. (4)) in MK-1 test. The Mann Kendall Z statistics were tested for significance levels with the threshold values.

3.2.6. Software packages

Two open source packages in R Version (3.5.3) namely “modifiedmk” (Patakamuri and O’Brien, 2019) and “HKprocess” (Tyralis, 2016) are used to perform MK tests. The modifiedmk was used to perform MK1, MK2, and MK3 tests and Sen’s slope test. Another package HKprocess is used to perform MK4 test. To get the spatial patterns of trends from point observations, the technique based on the kriging interpolation is implemented.

4. Results

Monthly, seasonal, and annual trends in rainfall and rainfall extremes are analyzed using four different MK tests (i.e., MK1/MK2/MK3/MK4) for 28 grids covering the Nagavali and Vamsadhara basins at a confidence level of 90% or higher. If any grid is showing either positive or negative trends in at least 3 tests, then it is considered as a threshold value and the trends of those grids are analyzed. The total number of grids showing significant trends (positive/negative) at a 90% confidence level are presented in Table 4. The spatial patterns of trends in rainfall and rainfall extremes are mapped using the kriging interpolation method for the Nagavali and Vamsadhara basins. Present research is

Table 4 Total number of IMD grids showing significant trends ($\geq 90\%$ confidence level) for rainfall and rainfall extremes in both Nagavali and Vamsadhara Basin.

	Rainfall			CDD			PRCPTOT			R10MM			R20MM			R40MM			R95PTOT			RX1DAY			RX5DAY		
	N+/ N-	V+/ V-		N+/ N-	V+/ V-		N+/ N-	V+/ V-		N+/ N-	V+/ V-		N+/ N-	V+/ V-		N+/ N-	V+/ V-		N+/ N-	V+/ V-		N+/ N-	V+/ V-		N+/ N-	V+/ V-	
Long-Term	Annual	2/1	7/0	2/0	2/0	2/1	7/0	2/1	7/0	4/1	6/1	4/0	0/0	5/0	1/0	4/0	0/0	0/0	5/0	1/0	4/0	0/0	0/0	1/0	2/0	0/0	2/0
	Winter	0/4	0/3	0/3	0/1	0/4	0/1	0/8	0/1	0/1	0/0	0/0	0/2	0/0	0/2	0/0	0/2	0/0	0/0	0/0	0/1	0/0	0/1	0/2	0/6	0/6	0/6
	Pre-Monsoon	2/0	9/0	0/4	0/7	0/1	2/0	5/0	3/0	4/0	2/0	4/0	0/0	2/0	7/0	0/0	7/0	0/0	2/0	2/0	3/0	3/0	3/0	8/0	0/0	9/0	0/0
	Monsoon	5/1	9/1	2/0	2/4	2/1	5/0	9/2	2/2	8/0	5/1	8/0	6/1	6/0	4/1	6/0	6/1	6/0	6/0	4/1	6/0	3/1	2/0	1/1	7/0	0/0	7/0
Pre-1950	Post-Monsoon	0/1	0/0	3/0	1/0	0/0	0/1	0/1	0/1	0/1	0/0	0/0	0/0	0/0	0/0	0/0	0/0	0/0	0/0	0/0	0/0	0/0	0/0	0/0	0/0	0/0	0/0
	Annual	0/0	0/0	0/0	0/0	0/0	0/0	2/0	2/0	0/0	0/0	0/1	0/0	0/1	0/0	0/1	0/0	0/0	0/1	0/1	0/0	0/1	0/0	0/0	0/0	0/0	0/0
	Winter	0/0	0/0	0/0	0/0	0/0	0/0	0/0	0/0	0/0	1/0	0/0	0/1	1/0	1/0	1/0	1/0	1/0	0/0	0/0	0/4	0/0	0/0	0/0	0/0	0/1	0/0
	Pre-Monsoon	2/0	0/0	0/0	0/0	9/0	0/0	4/0	4/0	3/0	3/0	0/0	0/0	0/0	0/0	0/0	0/0	0/0	0/0	0/0	0/0	2/0	3/0	5/0	0/0	0/0	0/0
Post-1950	Monsoon	0/0	0/3	0/0	0/0	2/0	0/2	0/0	0/3	0/0	0/0	0/1	0/0	0/1	0/0	0/1	0/0	0/1	0/0	0/0	0/1	0/0	0/0	0/0	0/0	0/2	0/0
	Post-Monsoon	2/0	0/0	0/0	0/0	10/0	0/1	4/0	4/0	2/0	3/0	2/0	2/0	2/0	2/0	2/0	2/0	2/0	0/0	0/0	0/0	2/0	3/0	5/0	0/0	0/0	0/0
	Annual	0/2	2/0	1/0	0/0	1/10	0/2	2/0	1/5	3/2	0/1	1/0	2/1	1/0	2/1	1/0	2/1	1/0	2/1	2/1	1/0	1/2	2/0	2/0	0/0	0/0	0/0
	Winter	0/0	0/0	0/0	0/0	0/0	0/0	0/0	0/0	0/0	0/0	0/0	0/0	0/0	0/0	0/0	0/0	0/0	0/0	0/0	0/0	0/0	0/0	0/0	0/0	0/0	0/0
Total	Pre-Monsoon	0/4	0/1	0/0	0/0	0/6	0/6	0/4	0/1	0/6	0/4	5/0	12/0	0/0	1/0	0/0	0/0	0/0	0/0	0/0	1/0	0/0	0/0	0/0	0/0	0/0	0/0
	Monsoon	0/3	6/0	2/1	2/1	0/10	0/2	6/0	1/5	6/1	3/0	0/1	3/0	1/2	1/0	2/2	3/0	2/2	1/2	1/0	1/0	2/2	3/0	0/2	4/0	0/0	4/0
	Post-Monsoon	0/3	0/1	0/0	0/0	0/7	0/5	0/4	0/1	0/5	0/1	0/0	0/1	0/0	0/0	0/0	0/1	0/0	0/0	0/0	1/0	3/0	0/0	0/0	0/0	0/0	0/1
	Annual	13/19	33/9	10/8	7/13	26/40	16/23	16/17	29/7	19/31	39/17	16/8	29/7	21/5	32/4	17/5	20/19	22/6	20/19	22/6	20/19	14/7	22/19	22/6	12/7	22/6	22/10

Note: N indicates Nagavali Basin, V indicates Vamsadhara Basin, + sign indicates number of grids showing increasing trend, - sign indicates number of grids showing decreasing trend.

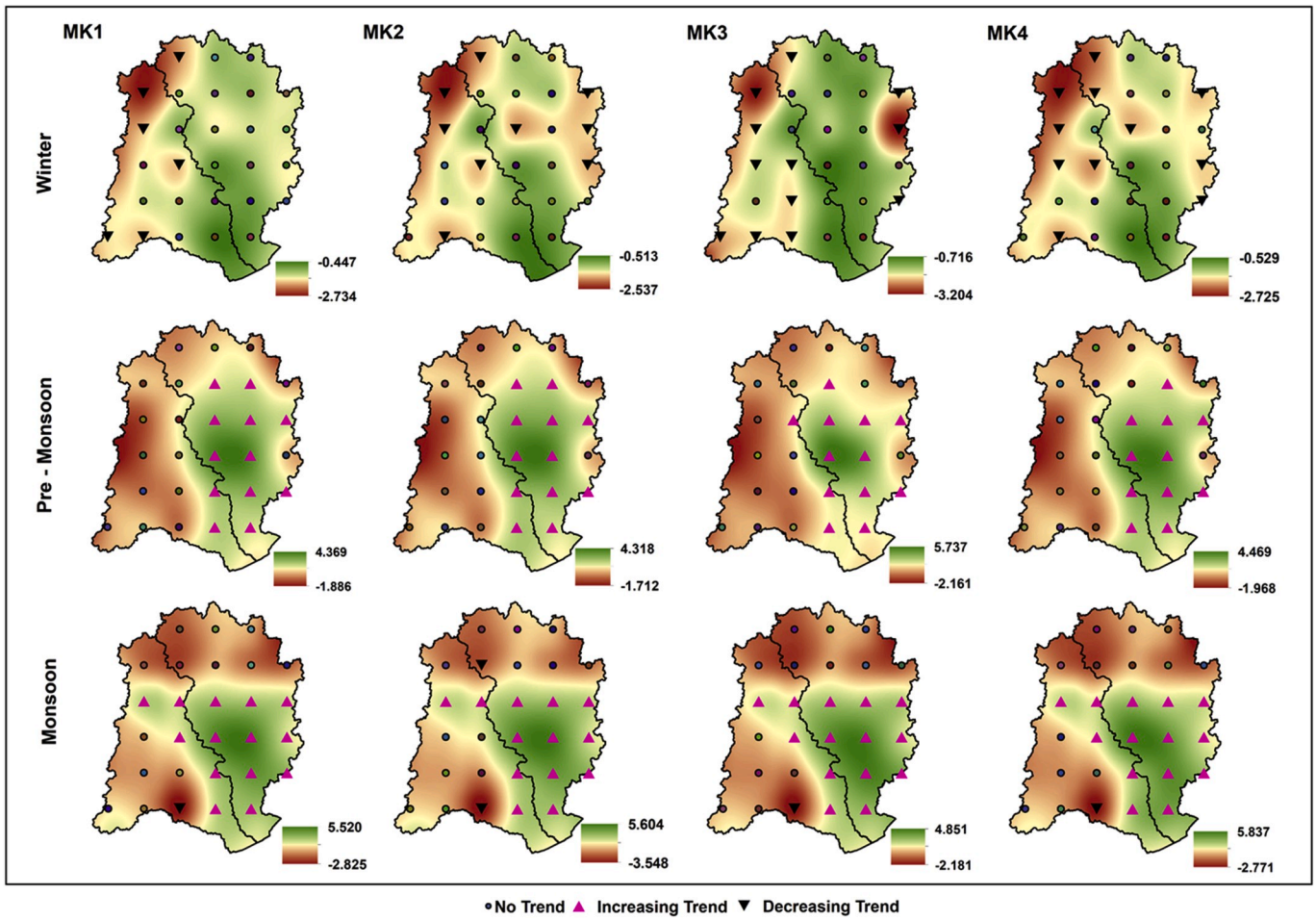


Fig. 2. Spatial plot of trends in rainfall during winter, pre-Monsoon and monsoon seasons.

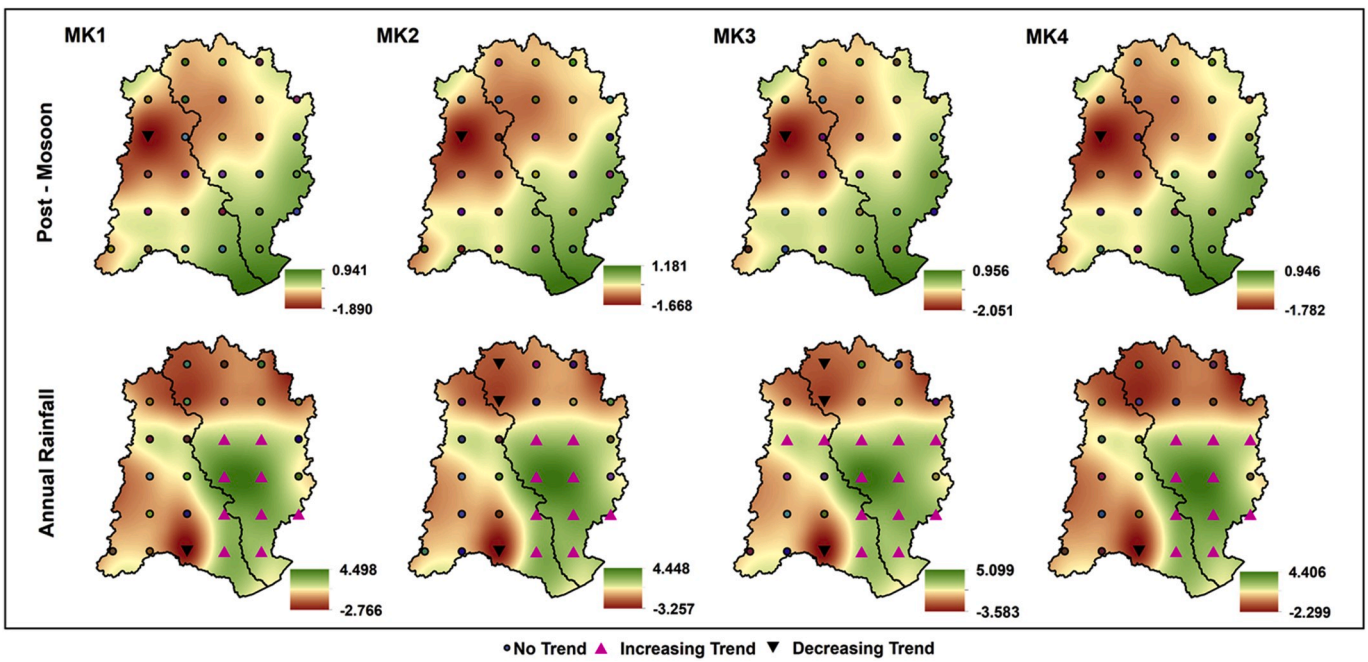


Fig. 3. Spatial plot of trends in post - monsoon rainfall and annual rainfall.

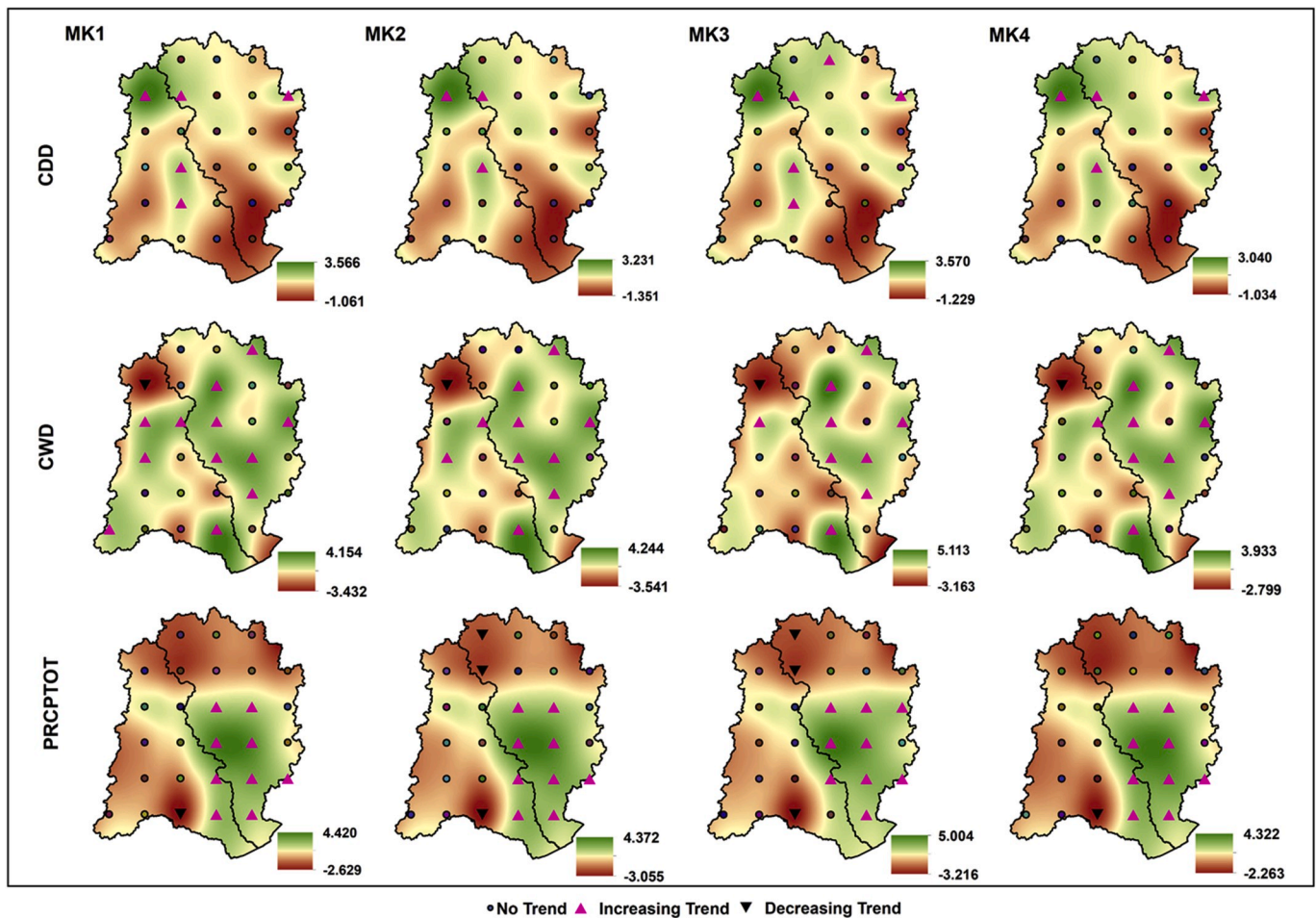


Fig. 4. Spatial plot of trends in annual rainfall extremes (CDD, CWD, and PRCPOT).

mainly focused on planning and management of water resources in the study river basins for agriculture and flood management. Hence, the detailed analysis of the annual and seasonal results are presented in the following sections and the monthly results are presented in supplementary material.

4.1. Trends in seasonal and annual rainfall

4.1.1. Long-term trends (1901–2018)

The Z statistics of the trends in seasonal (i.e., winter, pre-monsoon, monsoon, and post-monsoon) and annual rainfall are evaluated and presented in [Supplementary Table S1](#). As illustrated, 4 out of 12 grids in the Nagavali basin and 3 out of 16 grids in the Vamsadhara basin showed negative trends in the winter season. In the pre-monsoon and monsoon seasons, positive trends are observed in both the basins. The anecdotal evidence for the positive trends in pre-monsoon can be tied to the landfall of cyclones in this region that are formed in the Bay of Bengal (BoB) ([Uddin et al., 2019](#)). It is observed that the grids that are showing significant trends (positive/negative) in the pre-monsoon and monsoon seasons have also shown some similar trends at the annual scale. (Figs. 2 and 3). Whereas, in the post-monsoon season, a negative trend is observed in the Nagavali basin and no significant trend is observed in the Vamsadhara basin.

The spatial patterns of trends in seasonal and annual rainfall using four MK tests are presented in [Figs. 2 and 3](#). From these figures, it is evident that the grids with decreasing trends in winter are present in both the basins except at the lower portion of the Vamsadhara basin. However, no significant trend was found in the northern parts of the

Vamsadhara basin. The grids with increasing trends in the pre-monsoon are present in the lower portion of the Nagavali basin and at all locations in the Vamsadhara basin. Due to barotropic and baroclinic instabilities caused by tropical depressions formed in the BoB and their interactions with mean monsoonal flow ([Krishnamurthy et al., 2009](#)), the grids showing increasing trends in monsoon and annual rainfall are present in the lower and middle portions of both the basins. Whereas, in the post-monsoon season decreasing trends are present in the middle of the Nagavali basin.

4.1.2. Pre – 1950 (1901–1950) period

The Z statistics of trends in the seasonal and annual rainfall for pre-1950 are evaluated and presented in [Supplementary Table S2](#). In Nagavali basin, an increasing trend is observed at grids NG6 and NG11 in the pre-monsoon season and no obvious trends are found in rest of the seasons and in annual scale. In Vamsadhara basin, a decreasing trend is observed in the monsoon season and no significant trend is observed in other seasons and in annual scale.

From the spatial patterns it is observed that, the grids showing increasing trend in the pre-monsoon season are present at the middle and upper portions of the Nagavali basin. Whereas in Vamsadhara basin, the grids with decreasing trend are present in the middle portion of the basin.

4.1.3. Post-1950 (1951–2018) period

The Z statistics of trends in seasonal and annual rainfall for post-1950 period are evaluated and presented in [Supplementary Table S2](#). In the winter season, no significant trends are observed in both the basins.

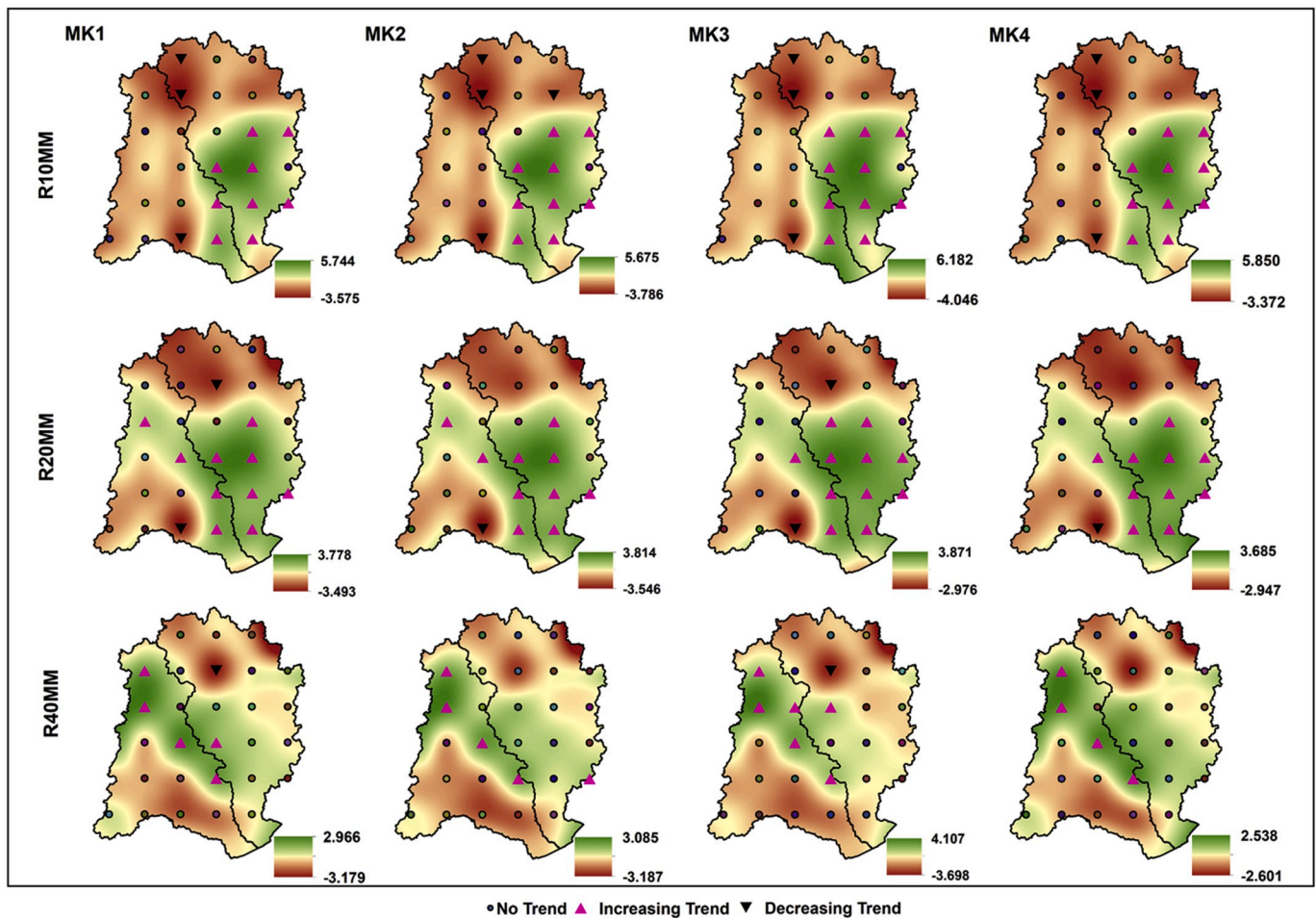


Fig. 5. Spatial plot of trends in annual rainfall extremes (R10MM, R20MM, and R40MM).

Except winter season, a decreasing trend is observed in Nagavali basins in all other seasons and in annual scale. In Vamsadhara basin, a decreasing trend is observed at grid VG13 in both the pre- and post-monsoon seasons. Whereas, an increasing trend is observed in the monsoon season and in annual scale.

The spatial patterns trends in seasonal and annual rainfall for the period of post-1950 are presented in [Supplementary Figs. S1 and S2](#). From these figures, it is evident that the grids showing decreasing trend in the pre-monsoon are present in the lower and middle portions of the Nagavali basin and at the upper portion of the Vamsadhara basin. Whereas, in the post-monsoon, the grids with decreasing trend are presented in all portions of the Nagavali basin and upper portion of the Vamsadhara basin. In the monsoon season, the grids showing decreasing trends in Nagavali basin are present at lower and middle portions of the basin whereas, in Vamsadhara the grids with increasing trend are present all over the basin. The grids showing decreasing trends at annual scales in Nagavali basin are present at middle and lower portions of the basins and the grids with increasing trend in Vamsadhara basin are present in the middle portion of the basin. The grids which showed significant trends in post-1950 in both the basins has shown similar trends in the overall period (i.e., 1901–2018) trend analysis.

4.2. Trends in rainfall extremes

4.2.1. Trends in annual rainfall extremes

The Z statistics of annual rainfall extremes at three time steps (i.e., long-term, pre-1950, and post-1950) are computed. However, only the Z statistics of long-term annual rainfall extremes are presented in the

[Supplementary Table S3](#). In pre-1950, no obvious trends are observed for all the extremes in both the basins. Whereas, in post-1950 an increasing trend for CDD and decreasing trend for all other rainfall extremes is observed in Nagavali basin. However, an increasing trend is observed for the extremes CWD, R10MM, R40MM, R95PTOT, and RX1DAY at very few grid points (i.e., ≤ 2). As validation, the results of R95PTOT are in good agreement with [Bisht et al. \(2018a\)](#). In the Vamsadhara basin, no significant trend is observed for the extremes CDD and RX5DAY. An increasing trend is observed for the extremes PRCPTOT, R20MM, R40MM, R95PTOT, and RX1DAY. However, CWD has shown decreasing trend and both the trends are observed for R10MM.

In Long-term, an increasing trend is observed for all the rainfall extremes in the Nagavali basin. However, a decreasing trend is observed at grid NG12 for CWD and at grid NG3 for PRCPTOT, R10MM, and R20MM in the Nagavali basin. In the Vamsadhara basin, no significant trend is observed for R40MM and RX1DAY. Whereas, an increasing trend is observed for other rainfall extremes. As validation, the trends in R95PTOT and RX5DAY are found to be in good agreement with [Bisht et al. \(2018a\)](#).

The spatial patterns of the trends in long-term annual rainfall extremes are presented in [Figs. 4–6](#). Increasing trends in CDD at a rate of 2 days/decade are present in the upper portion of both the basins and as expected the same grids showed a decreasing trend for CWD. Interestingly, the rate of decrease in CWD is also found to be the same. For the extremes, PRCPTOT, R10MM, and R20MM a decreasing trend is present in the lower portion of the Nagavali basin and the upper portion of the Vamsadhara basin. For CWD, the grids showing increasing trends are

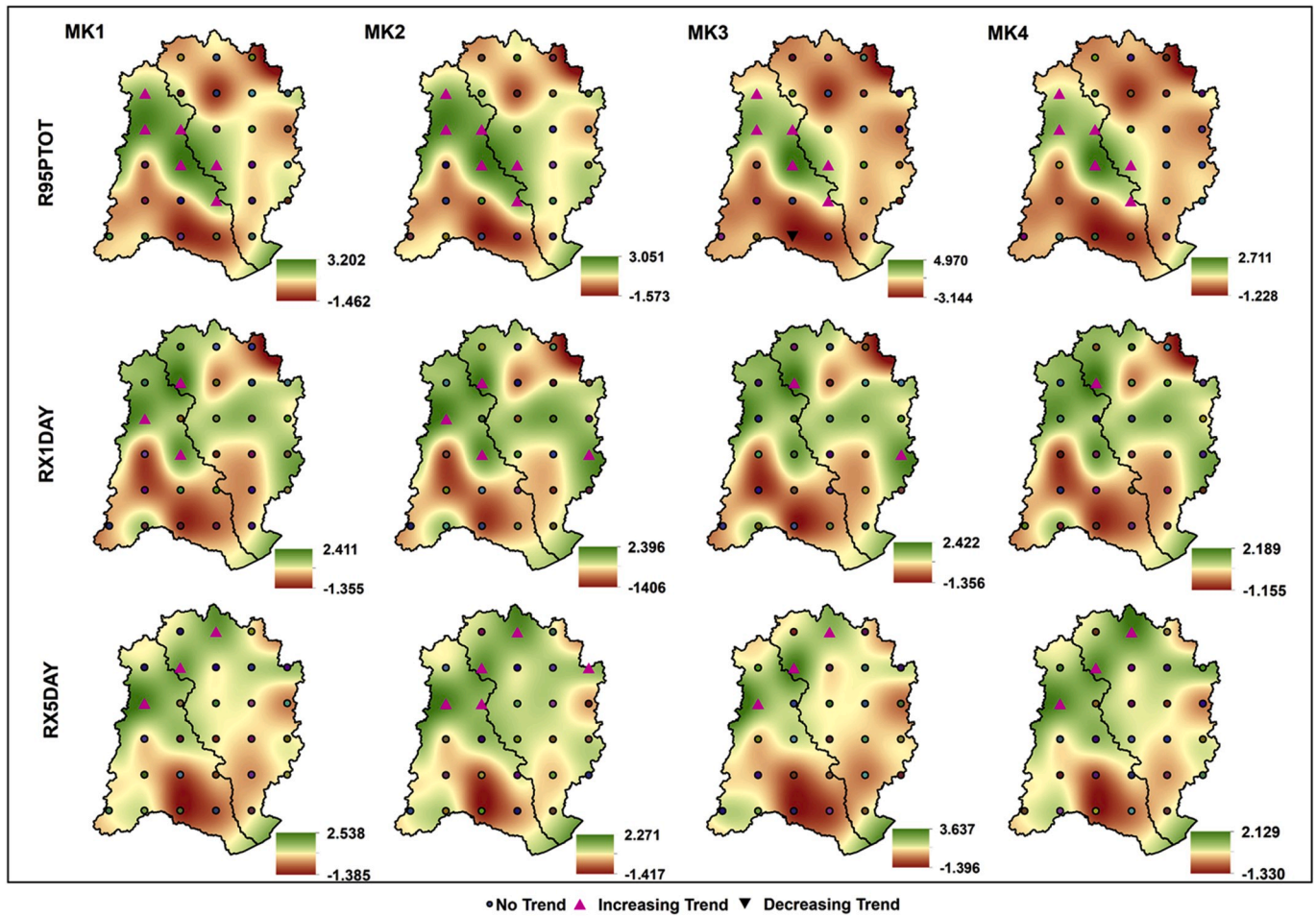


Fig. 6. Spatial plot of trends in annual rainfall extremes (R95PTOT, RX1DAY, and RX5DAY).

present in both the basins except at the upper portion of the Nagavali basin. The grids showing increasing trends for PRCPTOT, R10MM, and R20MM are present in the lower and middle portions of both the basins. For the extremes, R95PTOT, RX1DAY, and RX5DAY the increasing trends are present in the middle and upper portions of the Nagavali basin. In the Vamsadhara basin, the grids showing increasing trends for R95PTOT are present in the lower portion of the basin and for RX5DAY at the middle and upper portions of the basin because of cyclonic storms as they produce rainfall for more than 5 days (Dash et al., 2009).

4.2.2. Trends in seasonal rainfall extremes

The Z statistics of the rainfall extremes in the monsoon season are presented in Supplementary Table S4. In the winter season, no trend is evident for R40MM and R95PTOT in the Nagavali basin and R20MM in the Vamsadhara basin. Except CDD, a decreasing trend is observed for all the rainfall extremes in the winter season. In both the pre-monsoon and monsoon seasons, a positive trend is observed for all the rainfall extremes except for CDD and R10MM in the Vamsadhara basin and CWD in the Nagavali basin and NG3 in the monsoon season. In the Vamsadhara basin, a clear negative trend is observed for CDD in the pre-monsoon season. Whereas, in the monsoon season a negative trend is observed over 3 grids and a positive trend for 2 grids in the basin. For CWD in the Nagavali basin, a negative trend is observed at NG8 in the pre-monsoon and at NG12 in the monsoon. A positive trend is observed at NG4 and NG11 in the monsoon season. At grid NG3, a negative trend is observed for all the rainfall extremes except for CDD and CWD. For R10MM in the Vamsadhara basin, a clear positive trend is observed during the pre-monsoon season. Whereas, in the monsoon season a

positive trend is observed at 9 grids and a negative trend at 3 grids. No significant trend is observed for the rainfall extremes in the post-monsoon season except for CDD where it showed a positive trend for a few grids in both the basins.

The spatial patterns of rainfall extremes in all seasons are computed. However, only the spatial patterns of rainfall extremes for the monsoon season are presented in Figs. 7–9 and the spatial patterns of winter season are presented in Supplementary Figs. S6–S8. The grids showing increasing trends for CDD in the winter season can be seen in all parts of the Nagavali basin. For the extremes, CWD, R10MM, and RX1DAY the grids showing decreasing trends are present in most of the Nagavali basin. Whereas, for R95PTOT and RX5DAY a decreasing trend is present in the middle and upper portions of the Nagavali basin and in the middle for R20MM. In the Vamsadhara basin, the grids showing decreasing trends for CWD, R10MM, and PRCPTOT are present in the middle portion of the basin. For the extremes, R95PTOT and RX1DAY the grids showing decreasing trends are present in the upper portion of the basin and for R40MM and RX5DAY the grids are present in the middle and upper portions of the basin.

In the pre-monsoon season, the decreasing trend for CDD is present in both the basins except at the lower portion of the Vamsadhara basin. In the Nagavali basin, the grids with decreasing trends for CWD and increasing trends for PRCPTOT are present in the lower and middle portions. The increasing trends for R20MM, R95PTOT, and RX1DAY are present in the middle and upper portions of the Nagavali basin. For R40MM, increasing trends are in the upper portion of the basin. In the Vamsadhara basin, increasing trends are present in the entire basin except for CDD and CWD. For CWD, the grids showing increasing trends

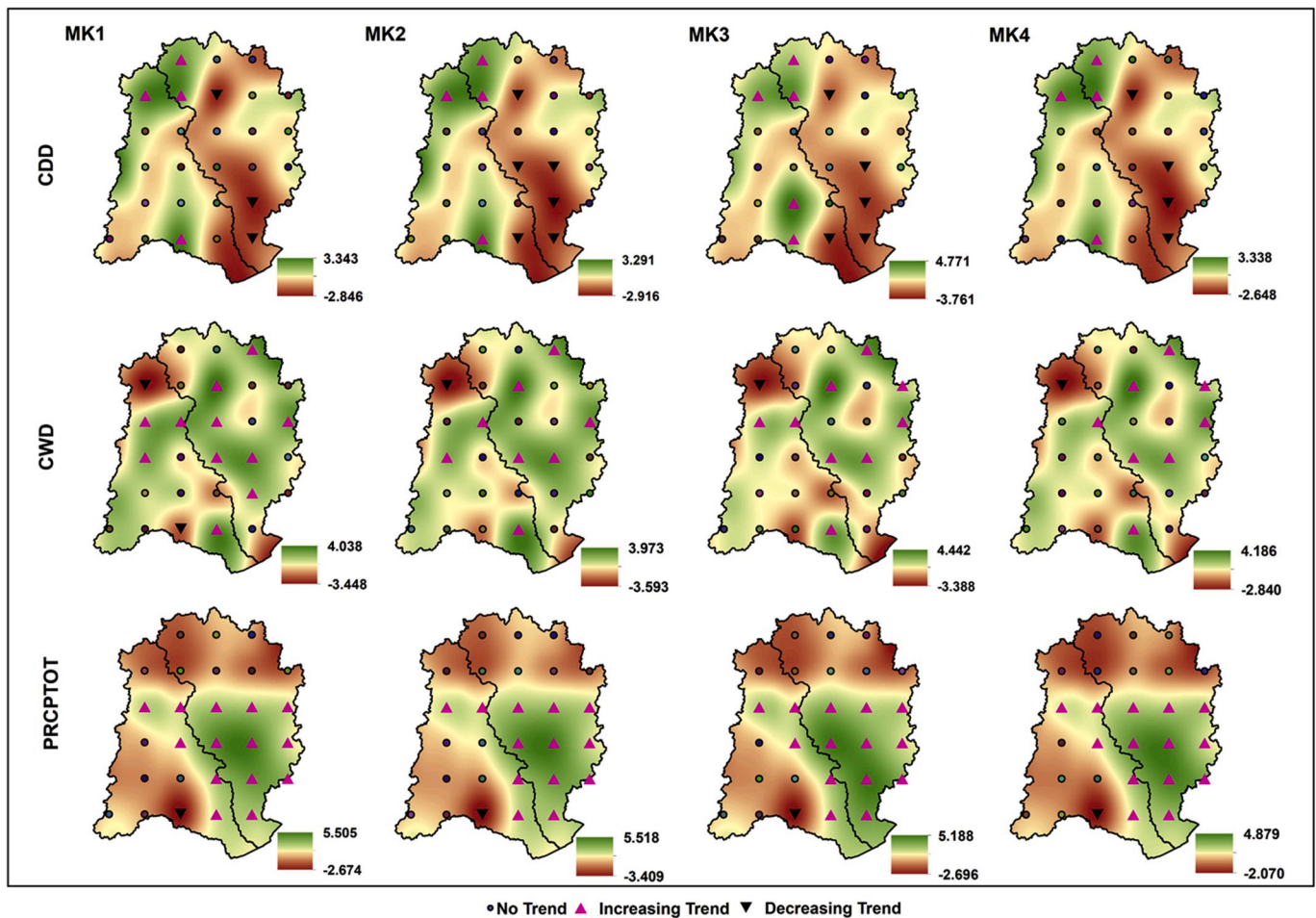


Fig. 7. Spatial plot of trends in rainfall extremes (CDD, CWD, and PRCPTOT) during Monsoon Season.

are present in the upper portion of the basin.

In the monsoon season, increasing trends with all rainfall extremes for all portions of the Nagavali basin are evident except at NG12 in the upper portion of the basin for CWD. Interestingly, grid NG3 in the lower portion of the Nagavali basin has shown a decreasing trend for all the rainfall extremes except for CDD. In the Vamsadhara basin, the increasing trend for all the rainfall extremes are present in the lower and middle portions of the basin except for CDD, CWD, and RX5DAY. CDD has shown a decreasing trend at few grids in all portions of the basin and an increasing trend at few grids in the upper portion of the basin. For CWD and RX5DAY, the grids showing increasing trends are present in the entire basin. In the upper portion of the Vamsadhara basin the grids showed a decreasing trend for R10MM. In the post-monsoon season, the grids are having an increasing trend for CDD in the middle and upper portions of the Nagavali basin and in the middle portion of the Vamsadhara basin.

In the post-monsoon season no significant trend is observed in rainfall extremes except for CDD where it showed increasing trend. The grids showing increasing trend are present in all parts of the Nagavali basin and upper portion of the Vamsadhara basin.

4.2.3. Trends in seasonal rainfall extremes in pre- and Post-1950 periods

In the winter season no significant trend is evident in pre- and post-1950 period for all the rainfall extremes in both the basins. In the pre-1950 period, an increasing trend is observed for most of the extremes in both the Nagavali and Vamsadhara basins in the pre- and post-monsoon seasons. Whereas, in post-1950 a decreasing trend is observed in the pre- and post-monsoon seasons. In the monsoon season,

in post-1950, a decreasing trend is observed in all the extremes in the Nagavali basin compared to pre-1950. Whereas, in Vamsadhara basin an increasing trend is observed in all the extremes in post-1950 where they showed decreasing trend in pre-1950. The detailed explanation about the spatial patterns of rainfall extremes in pre- and post-1950 are provided in supplementary material.

4.3. Magnitude of the trends

The magnitudes of rainfall and rainfall extremes are calculated using the Sen's slope method. It is observed that the annual rainfall in the Nagavali basin has increased at a rate of 2 mm/decade and in the Vamsadhara basin it has increased at a rate of 8.5 mm/decade in the last 118 years. The maximum rate of increase in seasonal rainfall is observed in the monsoon season. Rainfall in the monsoon season has also increased at a rate of 4 mm/decade in the Nagavali basin and 9 mm/decade in the Vamsadhara basin. A very slight increase or decrease in the magnitude of rainfall extremes is observed over decadal scales.

4.4. Drivers of rainfall variability

Both the Nagavali and Vamsadhara basins have shown significant trends in rainfall and rainfall extremes in the past 118 years at various temporal scales. The trend analysis has been carried out using high resolution daily gridded data. According to Klein Tank et al. (2006), changes in data observation practices and irregular spatial distribution of rainfall stations, inhomogeneities are introduced in the time series data which could impact the computation of extreme indices. Due to

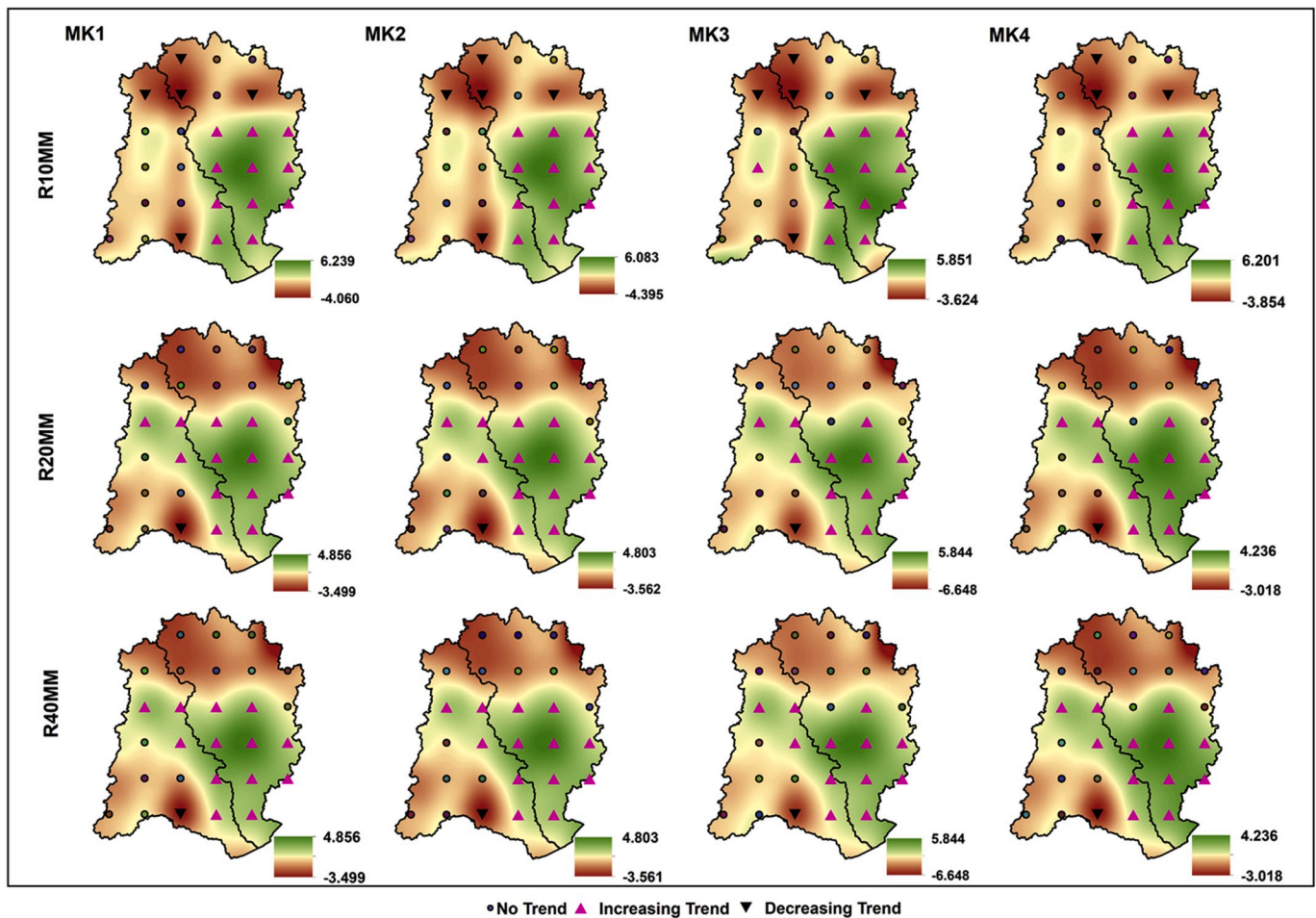


Fig. 8. Spatial plot of trends in rainfall extremes (R10MM, R20MM, and R40MM) during monsoon season.

this, there might be uncertainties in the trend analysis carried out using gridded products. In the present study, regions with higher density of rainfall stations has shown significant trends in both the Nagavali and Vamsadhara basins. It is also known that Bay of Bengal is one of the hot spots for the genesis of tropical cyclones which propagates either westwards or northwards playing a major in rainfall extremes (Krishnamurthy et al., 2009). Both the Nagavali and Vamsadhara basins are coastal basins and receive high rainfall in pre- and post-monsoon seasons. Hence, the results exhibited significant increasing trend in the pre-monsoon season.

Another possible reason for increasing trends in rainfall and rainfall extremes in both the basins is because of changes in land use and land cover. In the last three decades, the forest cover in the Nagavali basin has decreased rapidly because of urbanization (Rao et al., 2019). The increasing trend in the Nagavali basin may be attributed to the effect of urbanization, as Bisht et al. (2018a) suggested that the basin has shown a decreasing trend in the pre-urbanization era (1901–1970), an increasing trend in the post-urbanization era (1971–2015) and an increasing trend over the long term for both annual and monsoon rainfall. Whereas, in the Vamsadhara basin no significant changes in land use and land cover are found. Hence, the results from trend analysis results in the Vamsadhara basin for rainfall and rainfall extremes at various temporal scales are in good agreement with the existing literature.

With regard to spatial patterns in rainfall and rainfall extremes, the Vamsadhara basin has shown significant increasing trends in the lower and middle portion of the basin when compared with the Nagavali basin. These increasing trends may be attributed to the local convective

processes as well as the extreme topography of the region, as the Eastern Ghats are densely located in the middle and upper portions of the Vamsadhara basin.

5. Conclusions

In the present study, the spatial and temporal variations of trend in rainfall and rainfall extremes over the Nagavali and Vamsadhara basins are examined using the long-term rainfall time series at three time periods (i.e., long-term (1901–2018), pre-1950, and post-1950) which provides extensive information about variations in rainfall patterns over the basins. From the results, significant difference in the patterns of rainfall and rainfall extremes are observed in both the Nagavali and Vamsadhara basins during pre- and post-1950 periods. In the long-term trend analysis, an increasing trend is confirmed in rainfall and rainfall extremes in the monsoon season in both the basins as expected. Interestingly, increasing trends are observed in rainfall and rainfall extremes in the pre-monsoon. It may be possible because of landfall cyclones in this region that are formed in Bay of Bengal. From this hydroclimatic analysis, the assessment of onset of monsoon along the west coast region and its gradual progression towards the vast regions of the Indian continent can have profound impacts in understanding the rainfall characteristics and their role over water related-disasters for current and changing climatic conditions. The increasing trends in the lower and middle portions of both the basins is partly related to the urbanization and local land use and land cover changes. A vast majority of the people in both the basins are dependent on agriculture for their livelihoods, and the increasing trends in rainfall and rainfall extremes and the resulting

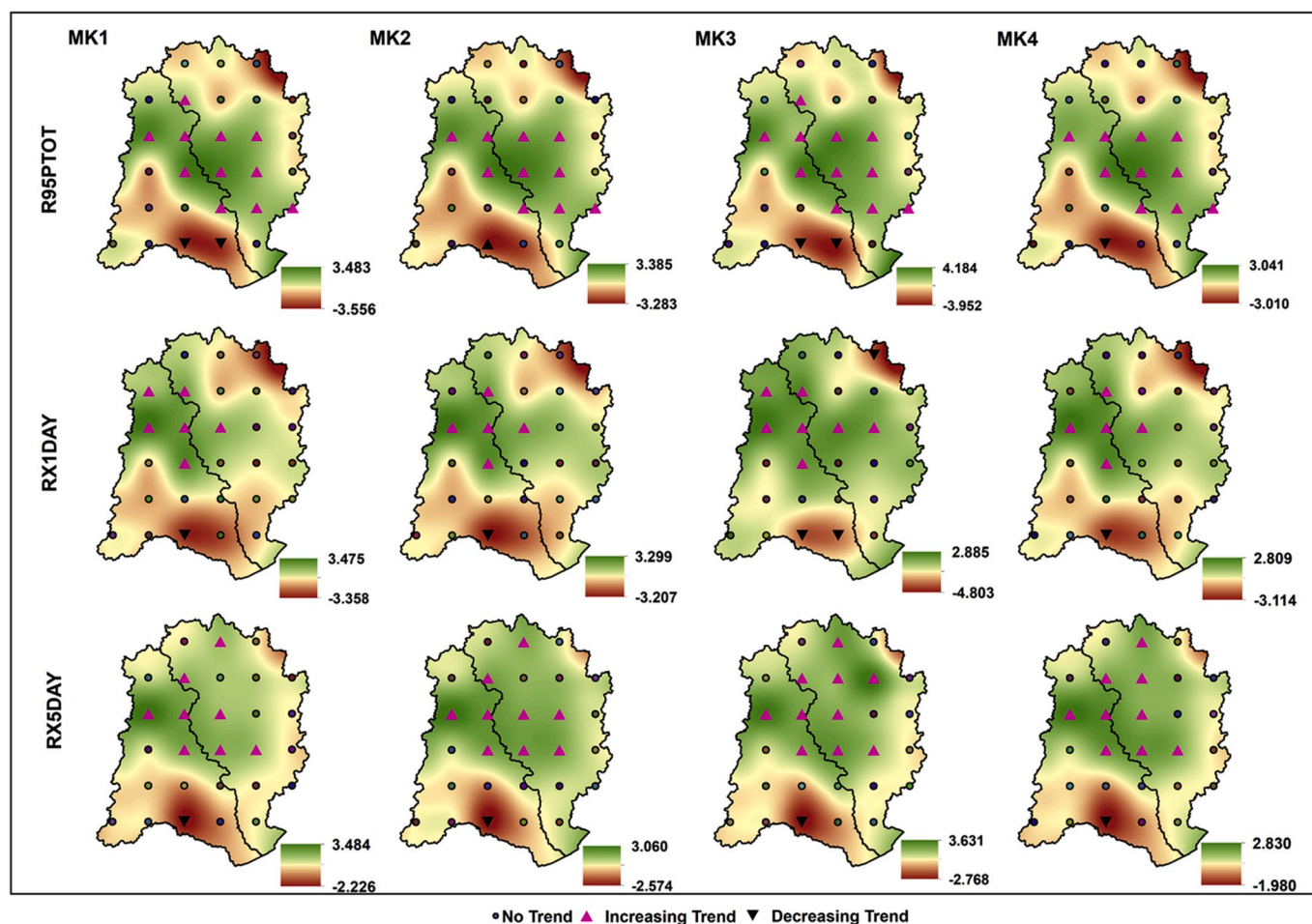


Fig. 9. Spatial plot of trends in rainfall extremes (R95PTOT, RX1DAY, and RX5DAY) during monsoon season.

recent flood events in this region deserves careful extension of this study into evaluating extreme hydrologic-hydraulic flow regimes. Findings from this study will be useful for developing and improving flood simulation models, agricultural operations and management, and understanding the streamflow characteristics for better management of available water resources in the basins.

Funding

The research described in this paper is carried out with fund by Ministry of Human Resource Development (MHRD), Government of India under Scheme for Promotion of Academic and Research Collaboration (SPARC) through project number P270. The fourth author's (V. Sridhar) effort was funded in part by the Virginia Agricultural Experiment Station (Blacksburg) and through the Hatch Program of the National Institute of Food and Agriculture at the United States Department of Agriculture (Washington, DC).

Declaration of competing interest

The authors declare that they have no known competing financial interests or personal relationships that could have appeared to influence the work reported in this paper.

CRedit authorship contribution statement

G. Venkata Rao: Data curation, Formal analysis, Investigation, Methodology, Software, Visualization, Writing - original draft, Writing -

review & editing. **K. Venkata Reddy:** Conceptualization, Data curation, Funding acquisition, Investigation, Methodology, Project administration, Resources, Software, Validation, Visualization, Writing - original draft, Writing - review & editing. **Raghavan Srinivasan:** Conceptualization, Funding acquisition, Investigation, Software, Supervision, Validation, Writing - review & editing. **Venkataramana Sridhar:** Conceptualization, Funding acquisition, Investigation, Software, Supervision, Validation, Writing - review & editing. **N.V. Umamahesh:** Funding acquisition. **Deva Pratap:** Funding acquisition.

Appendix A. Supplementary data

Supplementary data to this article can be found online at <https://doi.org/10.1016/j.wace.2020.100265>.

References

- Adarsh, S., Janga Reddy, M., 2015. Trend analysis of rainfall in four meteorological subdivisions of southern India using nonparametric methods and discrete wavelet transforms. *Int. J. Climatol.* 35, 1107–1124. <https://doi.org/10.1002/joc.4042>.
- Bisht, D.S., Chatterjee, C., Raghuvanshi, N.S., Sridhar, V., 2018a. Spatio-temporal trends of rainfall across Indian river basins. *Theor. Appl. Climatol.* 132, 419–436. <https://doi.org/10.1007/s00704-017-2095-8>.
- Bisht, D.S., Chatterjee, C., Raghuvanshi, N.S., Sridhar, V., 2018b. An analysis of precipitation climatology over Indian urban agglomeration. *Theor. Appl. Climatol.* 133, 421–436. <https://doi.org/10.1007/s00704-017-2200-z>.
- Bronaugh, D., 2019. PCIC implementation of climdex routines [WWW document]. URL: <https://cran.r-project.org/web/packages/climdex.pcic/climdex.pcic.pdf>.
- Dash, S.K., Kulkarni, M.A., Mohanty, U.C., Prasad, K., 2009. Changes in the characteristics of rain events in India. *J. Geophys. Res. Atmos.* 114. <https://doi.org/10.1029/2008JD010572>.

- Deshpande, N.R., Kothawale, D.R., Kulkarni, A., 2016. Changes in climate extremes over major river basins of India. *Int. J. Climatol.* 36, 4548–4559. <https://doi.org/10.1002/joc.4651>.
- Dhar, O.N., Nandargi, S., 2003. Hydrometeorological aspects of floods in India. *Nat. Hazards* 28, 1–33. <https://doi.org/10.1023/A:1021199714487>.
- Dubey, S.K., Sharma, D., 2018. Spatio-temporal trends and projections of climate indices in the banas river basin, India. *Environ. Process.* 5, 743–768. <https://doi.org/10.1007/s40710-018-0332-5>.
- Ghosh, S., Das, D., Kao, S.C., Ganguly, A.R., 2012. Lack of uniform trends but increasing spatial variability in observed Indian rainfall extremes. *Nat. Clim. Change* 2, 86–91. <https://doi.org/10.1038/nclimate1327>.
- Goswami, B.N., Venugopal, V., Sengupta, D., Madhusoodanan, M.S., Xavier, P.K., 2006. Increasing trend of extreme rain events over India in a warming environment. *Science* 314, 1442–1445. <https://doi.org/10.1126/science.1132027>.
- Guhathakurta, P., Menon, P., Inkane, P.M., Krishnan, U., Sable, S.T., 2017. Trends and variability of meteorological drought over the districts of India using standardized precipitation index. *J. Earth Syst. Sci.* 126, 1–18. <https://doi.org/10.1007/s12040-017-0896-x>.
- Guhathakurta, P., Rajeevan, M., 2008. Trends in the rainfall pattern over India. *Int. J. Climatol.* 28, 1453–1469. <https://doi.org/10.1002/joc.1640>.
- Guhathakurta, P., Rajeevan, M., Sikka, D.R., Tyagi, A., 2015. Observed changes in southwest monsoon rainfall over India during 1901–2011. *Int. J. Climatol.* 35, 1881–1898. <https://doi.org/10.1002/joc.4095>.
- Guhathakurta, P., Sreejith, O.P., Menon, P.A., 2011. Impact of climate change on extreme rainfall events and flood risk in India. *J. Earth Syst. Sci.* 120, 359–373. <https://doi.org/10.1007/s12040-011-0082-5>.
- Hamed, K.H., 2008. Trend detection in hydrologic data: the Mann-Kendall trend test under the scaling hypothesis. *J. Hydrol.* 349, 350–363. <https://doi.org/10.1016/j.jhydrol.2007.11.009>.
- Hamed, K.H., Rao, R.A., 1998. A modified Mann-Kendall trend test for autocorrelated data. *J. Hydrol.* 204, 182–196. [https://doi.org/10.1016/S0022-1694\(97\)00125-X](https://doi.org/10.1016/S0022-1694(97)00125-X).
- Hurst, H.E., 1951. Long-term storage capacity of reservoir. *Trans. Am. Soc. Civ. Eng.* 116, 770–799.
- Jain, S.K., Nayak, P.C., Singh, Y., Chandniha, S.K., 2017. Trends in rainfall and peak flows for some river basins in India. *Curr. Sci.* 112, 1712–1726. <https://doi.org/10.18520/cs/v112/i08/1712-1726>.
- Jaiswal, R.K., Lohani, A.K., Tiwari, H.L., 2015. Statistical analysis for change detection and trend assessment in climatological parameters. *Environ. Process.* 2, 729–749. <https://doi.org/10.1007/s40710-015-0105-3>.
- Jayadas, A., Ambujam, N.K., 2019. Observed trends in indices for daily rainfall extremes specific to the agriculture sector in Lower Vellar River sub-basin, India: extreme rainfall trends over Lower Vellar sub-basin. *J. Earth Syst. Sci.* 128 <https://doi.org/10.1007/s12040-019-1074-0>.
- Klein Tank, A.M.G., Peterson, T.C., Quadir, D.A., Dorji, S., Zou, X., Tang, H., Santhosh, K., Joshi, U.R., Jaswal, A.K., Kolli, R.K., Sikder, A.B., Deshpande, N.R., Revadekar, J.V., Yeleuova, K., Vandasheva, S., Paleyeva, M., Gomboluudev, P., Budhathoki, K.P., Hussain, A., Afzaal, M., Chandrapala, L., Anvar, H., Amanmurad, D., Asanova, V.S., Jones, P.D., New, M.G., Spektorman, T., 2006. Changes in daily temperature and precipitation extremes in central and south Asia. *J. Geophys. Res.* 111, D16105. <https://doi.org/10.1029/2005JD006316>.
- Krishnamurthy, C.K.B., Lall, U., Kwon, H.H., 2009. Changing frequency and intensity of rainfall extremes over India from 1951 to 2003. *J. Clim.* 22, 4737–4746. <https://doi.org/10.1175/2009JCLI2896.1>.
- Kumar, S., Merwade, V., Kam, J., Thurner, K., 2009. Streamflow trends in Indiana: effects of long term persistence, precipitation and subsurface drains. *J. Hydrol.* 374, 171–183. <https://doi.org/10.1016/j.jhydrol.2009.06.012>.
- Kumar, V., Jain, S.K., Singh, Y., 2010. Analysis of long-term rainfall trends in India. *Hydrol. Sci. J.* 55, 484–496. <https://doi.org/10.1080/02626667.2010.481373>.
- Pai, D.S., Sridhar, L., Rajeevan, M., Sreejith, O.P., Satbhai, N.S., Mukhopadhyay, B., 2014. Development of a new high spatial resolution (0.25° × 0.25°) long period (1901–2010) daily gridded rainfall data set over India and its comparison with existing data sets over the region. *Mausam* 65, 1–18.
- Patakamuri, S.K., O'Brien, N., 2019. Modified versions of Mann Kendall and spearman's rho trend tests [WWW document]. URL: <https://cran.r-project.org/web/packages/modifieddmk/modifieddmk.pdf>.
- Rajeevan, M., Bhat, J., Jaswal, A.K., 2008. Analysis of variability and trends of extreme rainfall events over India using 104 years of gridded daily rainfall data. *Geophys. Res. Lett.* 35, 1–6. <https://doi.org/10.1029/2008GL035143>.
- Rao, G.R., Mounika, K.S.S., Rao, M.J., 2019. Change detection analysis of Vamsadhara - Nagavali river fluvial system, using multi-temporal remote sensing data and GIS techniques. *Int. J. Adv. Remote Sens. GIS* 8, 2955–2962. <https://doi.org/10.23953/cloud.ijars.404>.
- Roy, S. Sen, Balling, R.C., 2004. Trends in extreme daily precipitation indices in India. *Int. J. Climatol.* 24, 457–466. <https://doi.org/10.1002/joc.995>.
- Seneviratne, S.I., Nicholls, N., 2012. Changes in Climate Extremes and Their Impacts on the Natural Physical Environment. In: *Managing the Risks of Extreme Events and Disasters to Advance Climate Change Adaptation: Special Report of the Intergovernmental Panel on Climate Change*, pp. 339–392. <https://doi.org/10.1017/CBO9781139177245.009>.
- Seong, C., Sridhar, V., 2017. Hydroclimatic variability and change in the Chesapeake Bay watershed. *J. Water Clim. Chang.* 8, 254–273. <https://doi.org/10.2166/wcc.2016.008>.
- Sharma, P.J., Loliyana, V.D., Resmi, S.R., Timbadiya, P.V., Patel, P.L., 2018. Spatiotemporal trends in extreme rainfall and temperature indices over Upper Tapi Basin, India. *Theor. Appl. Climatol.* 134, 1329–1354. <https://doi.org/10.1007/s00704-017-2343-y>.
- Sridhar, V., Jin, X., Jaksa, W.T.A., 2013. Explaining the hydroclimatic variability and change in the Salmon River basin. *Clim. Dynam.* 40, 1921–1937. <https://doi.org/10.1007/s00382-012-1467-0>.
- Sridhar, V., Modi, P., Billal, M.M., Valayamkunnath, P., Goodall, J.L., 2019. Precipitation extremes and flood frequency in a changing climate in southeastern Virginia. *J. Am. Water Resour. Assoc.* 55, 780–799. <https://doi.org/10.1111/1752-1688.12752>.
- Su, L., Miao, C., Kong, D., Duan, Q., Lei, X., Hou, Q., Li, H., 2018. Long-term trends in global river flow and the causal relationships between river flow and ocean signals. *J. Hydrol.* <https://doi.org/10.1016/j.jhydrol.2018.06.058>.
- Tyrallis, H., 2016. *Hurst-kolmogorov Process Version*.
- Uddin, M.J., Li, Y., Cheung, K.K., Nasrin, Z.M., Wang, H., Wang, L., Gao, Z., 2019. Rainfall Contribution of Tropical Cyclones in the Bay of Bengal between 1998 and 2016 Using TRMM Satellite Data. *Atmosphere* vol. 10. <https://doi.org/10.3390/atmos10110699>.
- Vittal, H., Karmakar, S., Ghosh, S., 2013. Diametric changes in trends and patterns of extreme rainfall over India from pre-1950 to post-1950. *Geophys. Res. Lett.* 40, 3253–3258. <https://doi.org/10.1002/grl.50631>.
- Weldegerima, T.M., Zeleke, T.T., Birhanu, B.S., Zaitchik, B.F., Fetene, Z.A., 2018. Analysis of rainfall trends and its relationship with SST signals in the lake tana basin, Ethiopia. *Adv. Meteorol.* <https://doi.org/10.1155/2018/5869010>, 2018.
- Yadav, R., Tripathi, S.K., Pranuthi, G., Dubey, S.K., 2014. Trend analysis by Mann-Kendall test for precipitation and temperature for thirteen districts of Uttarakhand. *J. Agrometeorol.* 16, 164–171.
- Yang, M., Chen, X., Cheng, C.S., 2016. Hydrological impacts of precipitation extremes in the huaihe river basin, China. *SpringerPlus* 5, 1–13. <https://doi.org/10.1186/s40064-016-3429-1>.
- Yue, S., Pilon, P., Phinney, B., 2003. Canadian streamflow trend detection: impacts of serial and cross-correlation. *Hydrol. Sci. J.* 48, 51–64. <https://doi.org/10.1623/hysj.48.1.51.43478>.